



E(5)-like emerging γ softness in ^{82}Kr Chunxiao Zhou ^{1,2,*} and Tao Wang ^{3,†}¹*College of Mathematics and Physics Science, Hunan University of Arts and Science, Changde 415000, People's Republic of China*²*Hunan Province Key Laboratory of Photoelectric Information Integration and Optical Manufacturing Technology, Changde 415000, People's Republic of China*³*College of Physics, Tonghua Normal University, Tonghua 134000, People's Republic of China*

(Received 15 February 2023; revised 30 July 2023; accepted 3 August 2023; published 16 August 2023)

Recently the interacting boson model with SU(3) higher-order interactions was proposed by one of the authors, in which new γ softness can emerge. This stimulates further discussion on the connections between the new γ softness and realistic γ -soft nuclei. In this paper, E(5)-like γ softness arises when the SU(3) fourth-order interaction $\hat{C}_2^2[\text{SU}(3)]$ is considered. The corresponding transitional behaviors are similar to those from the U(5) limit to the O(6) limit in the previous interacting boson model, IBM-1, which provides a novel perspective for understanding the new model. Low-lying spectra, $B(E2)$ values, and quadrupole moment of the first 2_1^+ state are investigated. The E(5)-like nucleus ^{82}Kr is exemplified, where the calculated low-lying level energies and the associated $B(E2)$ values fit very well with the experimental data.

DOI: [10.1103/PhysRevC.108.024309](https://doi.org/10.1103/PhysRevC.108.024309)**I. INTRODUCTION**

Nuclear shapes arising from collective dynamics between nucleons provide a fundamental concept to understand various properties of atomic nuclei [1]. Taking into account quadrupole degrees of freedom, nuclear shapes are characterized as a spherical harmonic vibrator [2], an axially symmetric deformed rotor [3] (prolate or oblate), a γ -unrelated rotor [4], or a γ -rigid triaxial rotor [5]. The nuclear shapes can be elegantly described in the framework of the interacting boson model (IBM) [6]. In the simplest version IBM-1, collective properties of nuclei can be well described by Hamiltonian with up to two-body interactions. Spectra of spherical [the U(5) limit], prolate [the SU(3) limit], oblate [the $\overline{\text{SU}}(3)$ limit], and γ -soft [the O(6) limit] nuclei can be reproduced, and shape transitional behaviors between the typical collective excitation modes are also extensively investigated in this model [7–17]. The abrupt shape transition between different paradigms is characterized as critical point symmetry (CPS) [18,19], which provides a simple parameter-free analytical treatment of transitional nuclei. In particular, the E(5) CPS [18] corresponds to the critical point of the transition from spherical to deformed γ -unstable shapes. This description was initially built within the Bohr-Mottelson (BM) model [1], where the collective potential function is taken as an infinite square well that only depends on β . Based on the correspondence between the BM model and IBM, relationships between the E(5) model and IBM are explored in [20,21].

It is worth noting that the Hamiltonian, which only contains the lower-order interactions, has some limitations in

describing the shapes. For example, it fails to account for the γ -rigid triaxial deformation [22], which means that the γ -rigid triaxial shape can not be treated on an equal footing with the prolate shape. The introduction of the higher-order interactions $[d^\dagger d^\dagger d^\dagger]^{(L)} \cdot [\tilde{d}\tilde{d}\tilde{d}]^{(L)}$ into the Hamiltonian can overcome this deficiency and induce a stable triaxial shape [23]. Meanwhile, it can be noticed that SU(3) symmetry-conserving higher-order interactions have been systematically investigated to remove the degeneracy of the γ band and the β band [24], and the rigid quantum asymmetric rotor within the SU(3) limit has been realized [25,26]. The SU(3) higher-order interactions were also investigated in [27–31]. Additionally, these interactions also play an important role in partial dynamical symmetry [32–34].

Inspired by the relationships between the γ -rigid triaxial deformation and the higher-order interactions [22,23], Fortunato *et al.* investigated triaxiality by introducing a cubic Q -consistent IBM Hamiltonian [35]. In the SU(3) limit, the cubic quadrupole interaction can describe the oblate shape, which can replace the oblate description of the $\overline{\text{SU}}(3)$ limit in previous IBM-1 and create a new evolution path from the prolate shape to the oblate shape. It opens a new door to understand the oblate shape in realistic nuclei. The analytically solvable prolate-oblate shape phase transitional description within the SU(3) limit was investigated [36], which offers a finite- N first-order shape transition.

These novel results [35,36] encourage us to understand the experimental phenomena from a new perspective. The interacting boson model with SU(3) higher-order interactions (SU3-IBM) proposed by one of the authors can give excellent explanations of the $B(E2)$ anomaly [37–41], where the anomaly phenomenon can be described by introducing the two SU(3) third-order interactions [42] or more higher-order interactions [43]. The Hamiltonian of the SU3-IBM is

*zhouchunxiao567@163.com

†suiyueqiaoqiao@163.com

constructed algebraically by only considering the U(5) limit and the SU(3) limit [44]. Various quadrupole deformations including the γ -rigid triaxiality can be described in the SU(3) limit, and the combination with the U(5) limit can induce the emergence of γ softness. This new γ softness was found to be intimately related to realistic γ -soft nuclei. For example, the normal states of ^{110}Cd can be described by the new γ -soft rotational mode [44], which is related to the spherical nucleus puzzle [45–53]. And this emerging γ softness can be also used to explain the properties of ^{196}Pt [54]. On the other hand, it is found that the SU3-IBM can describe the asymmetric prolate-oblate shape phase transition in the Hf-Hg region [55]. The belief that triaxiality results from the competition between the prolate shape and the oblate shape [44] is further exemplified, which is also discussed in the Xe-Ba region very recently [56].

The γ -softness discussed in the simplest SU3-IBM [44] has one specific feature that the energy of the 0_3^+ state is almost twice larger than the one of the 0_2^+ state, which is the major drawback when fitting the γ -soft nucleus of ^{196}Pt . This deficiency stimulates further investigations on the new γ softness. In this paper the fourth-order interaction $\hat{C}_2^2[\text{SU}(3)]$ is introduced and a new curious connection is established. Transitional behaviors similar to those from the U(5) limit to the O(6) limit are found, and γ softness with E(5) characteristic is demonstrated. Besides, the relationships between the irreps and shape deformations in the SU(3) limit are also discussed with the aim of realizing a rigid triaxial shape. Based on the SU3-IBM, the low-lying states and the $B(E2)$ values of ^{82}Kr are investigated, and it can be seen that the calculation results fit well with the experimental data [57].

The paper is organized as follows. In Sec. II, the Hamiltonian used in our paper is given. The level anticrossing and potential energy surface based on the new model are demonstrated in Sec. III. Section IV shows the transitional behaviors of the Hamiltonian including the excitation spectra, $B(E2)$ transition rates, and the quadrupole moment. In Sec. V, the calculation results of ^{82}Kr are compared with other theoretical results and experimental data. A summary of the main results and conclusions are given in Sec. VI.

II. HAMILTONIAN

The Hamiltonian supporting the new γ -softness was proposed in [44], and is composed of two parts. One is the d -boson number operator \hat{n}_d of the U(5) limit. Another term contains various symmetry-conserving interactions of the SU(3) limit. In Ref. [44] the SU(3) invariants are the second-order Casimir operator $-\hat{C}_2[\text{SU}(3)]$ and the third-order Casimir operator $\hat{C}_3[\text{SU}(3)]$, which describe the prolate shape and the oblate shape, respectively. Therefore, this formalism can be also used to the investigation of the prolate-oblate shape phase transition [58–60]. In previous research [44] the energy of the 0_3^+ state is larger than the experimental result. However, it can be noticed that the 0_3^+ state is close to the 0_2^+ state in many nuclei, such as ^{82}Kr [57,61]. In order to realize this characteristic, the fourth-order interaction $\hat{C}_2^2[\text{SU}(3)]$ is considered in this paper. Thus the Hamiltonian

is expressed as

$$\hat{H} = c \left[(1 - \eta)\hat{n}_d + \eta \left(-\frac{\hat{C}_2[\text{SU}(3)]}{2N} + \kappa \frac{\hat{C}_3[\text{SU}(3)]}{2N^2} + \xi \frac{\hat{C}_2^2[\text{SU}(3)]}{2N^3} \right) \right], \quad (1)$$

where c is the total fitting parameter, $0 \leq \eta \leq 1$, κ and ξ are the coefficients of the cubic and biquadrate interactions, respectively, and N is the boson number. If $\eta = 0$, it presents the spherical shape. If $\eta = 1$, it is a combination of the interactions in the SU(3) limit.

The two SU(3) Casimir operators are defined as

$$\hat{C}_2[\text{SU}(3)] = 2\hat{Q} \cdot \hat{Q} + \frac{3}{4}\hat{L} \cdot \hat{L}, \quad (2)$$

$$\hat{C}_3[\text{SU}(3)] = -\frac{4\sqrt{35}}{9}[\hat{Q} \times \hat{Q} \times \hat{Q}]^0 - \frac{\sqrt{15}}{2}[\hat{L} \times \hat{Q} \times \hat{L}]^0, \quad (3)$$

where \hat{Q} is the quadrupole momentum operator in the SU(3) limit and \hat{L} is the angular momentum operators. Under the group chain $U(6) \supset SU(3) \supset O(3)$, the eigenvalues of the Casimir operators can be expressed in terms of the SU(3) irreps (λ, μ) as

$$\langle \hat{C}_2[\text{SU}(3)] \rangle = \lambda^2 + \mu^2 + \lambda\mu + 3\lambda + 3\mu, \quad (4)$$

$$\langle \hat{C}_3[\text{SU}(3)] \rangle = \frac{1}{9}(\lambda - \mu)(2\lambda + \mu + 3)(\lambda + 2\mu + 3). \quad (5)$$

By containing higher-order interactions the Hamiltonian (1) can generate a collective potential of a stable axially asymmetric system [62] and is relevant to the anomaly phenomenon in nuclear structure [43].

To provide better descriptions for the new model, transitional behaviors from the U(5) limit to the SU(3) limit in the new model will be compared with those from the U(5) limit to the O(6) limit in the previous IBM-1 model. The Hamiltonian that describes the evolution from U(5) to O(6) can be expressed as

$$\hat{H}_0 = c \left[(1 - \eta)\hat{n}_d - \eta \frac{\hat{Q}_0 \cdot \hat{Q}_0}{N} \right], \quad (6)$$

where c is the total fitting parameter, $0 \leq \eta \leq 1$, and \hat{Q}_0 is the quadrupole operator in the O(6) limit. When $\eta = 0$, it describes the spherical shape of the U(5) limit. When $\eta = 1$, it corresponds to the γ softness of the O(6) limit.

III. LEVEL ANTICROSSING AND POTENTIAL ENERGY SURFACE

Compared to only considering second- and third-order interactions, the introduction of fourth-order interaction expands the choice of the lowest SU(3) irrep. For $N = 6$, the ground irrep can be represented by (4,4), which corresponds to shape variable $\gamma = 30^\circ$. To determine the values of ξ and κ in Eq. (1), the four lowest 0^+ states are plotted as a function of ξ and κ in the SU(3) limit, where ξ and κ are selected within the region corresponding to the irrep (4,4)

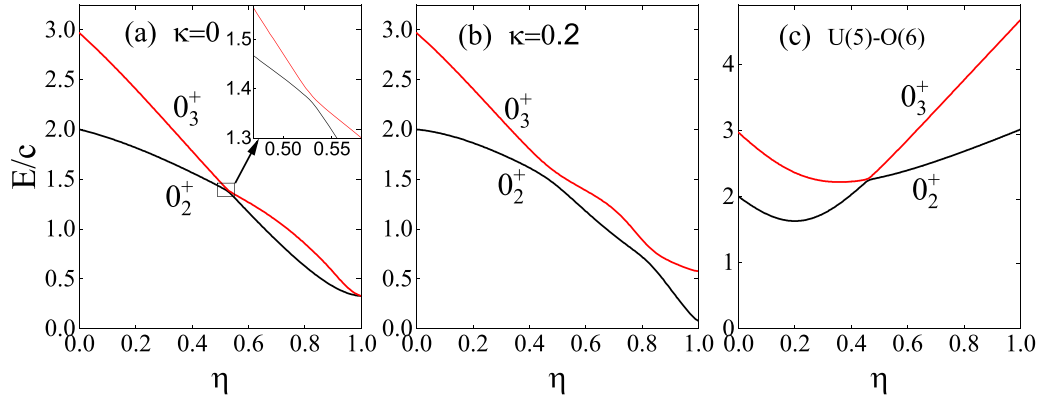


FIG. 1. Transitional behaviors of the 0_2^+ and 0_3^+ states as a function of η for $N = 6$, (a) from the U(5) limit to the SU(3) limit with $\xi = 0.2232$ and $\kappa = 0$, (b) from the U(5) limit to the SU(3) limit with $\xi = 0.2232$ and $\kappa = 0.2$, and (c) from the U(5) limit to the O(6) limit. Here panels (a) and (b) are obtained according to Eq. (1), while (c) corresponds to Eq. (6).

(as detailed in the Appendix). As shown in Fig. 1(a), when $\xi = 0.2232$ and $\kappa = 0$, the energy interval between the 0_2^+ and 0_3^+ states decreases with increasing η , and they exhibit crossing at $\eta = 0.53$. Here we want to point out that the level crossing in Fig. 1(a) is actually an anticrossing, which can be observed by enlarging the crossing-like point shown in the inset. Similar phenomena, which appear in first-order phase transitions due to the level repulsion, have been reported in [63,64]. The third-order interaction dissolves the crossing-like phenomenon and increase the energy interval between the

0_2^+ and 0_3^+ states as shown in Fig. 1(b). The level-crossing phenomenon of the 0_2^+ and 0_3^+ states has been regarded as a feature of the transitional behaviors from the U(5) limit to the O(6) limit [11] shown in Fig. 1(c). It is worth noting that the transitional behavior observed in the previous IBM-1 model is reproduced in the SU3-IBM, which is an appealing result and also a key feature sought by the new model.

In order to reveal the γ softness, the potential energy surface for the Hamiltonian (1) calculated using the ground state energy per boson in the large- N limit is [35,43]

$$\begin{aligned}
 V(\beta, \gamma) = & (1 - \eta) \frac{\beta^2}{1 + \beta^2} + \eta \left\{ -\frac{\beta^2}{2(1 + \beta^2)^2} [8 + \beta^2 + 4\sqrt{2}\beta \cos(3\gamma)] \right. \\
 & + \frac{\xi \beta^4}{2(1 + \beta^2)^4} [64 + 32\beta^2 + \beta^4 + 16\beta^2 \cos(6\gamma) + 8\sqrt{2}(8\beta + \beta^2) \cos(3\gamma)] \\
 & \left. + \frac{\kappa \beta^3}{9(1 + \beta^2)^3} [24\beta + 16\sqrt{2} \cos(3\gamma) + 6\sqrt{2}\beta^2 \cos(3\gamma) + \beta^3 \cos(6\gamma)] \right\}. \quad (7)
 \end{aligned}$$

For $N = 6$, the irrep of the ground state corresponding to $\gamma = 30^\circ$ in the SU(3) limit is (4,4); for the large- N limit, the corresponding irrep is $(\frac{2}{3}N, \frac{2}{3}N)$. According to Eq. (A3) in the Appendix, in the large- N limit $\xi = 0.375$ for $\kappa = 0$. The

contour plots of Eq. (7) with $\xi = 0.375$ are given in Figs. 2 for (a) $\kappa = 0$, (b) $\kappa = 0.2$, and (c) $\kappa = 0.6$, respectively. The γ values of the minimum points for $\kappa = 0$ and 0.2 are both 0° , which show the prolate shape. For $\kappa = 0.6$, the minimum

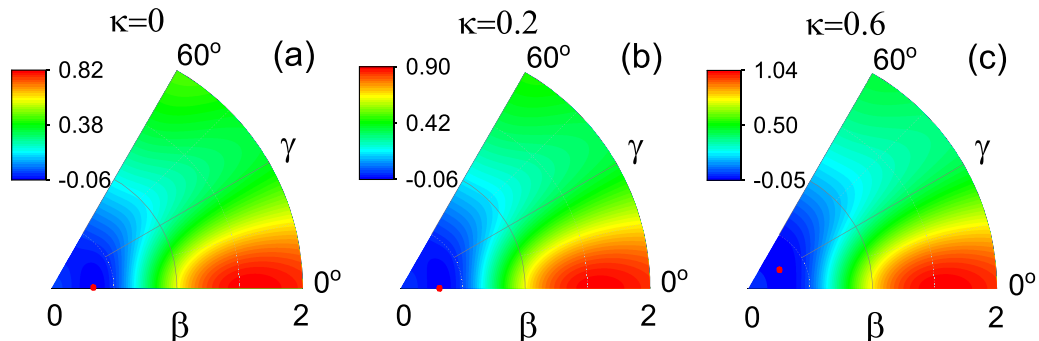


FIG. 2. Potential energy surfaces plotted in the large- N limit with $\xi = 0.375$, $\eta = 0.41$, (a) $\kappa = 0$, (b) $\kappa = 0.2$, (c) $\kappa = 0.6$.

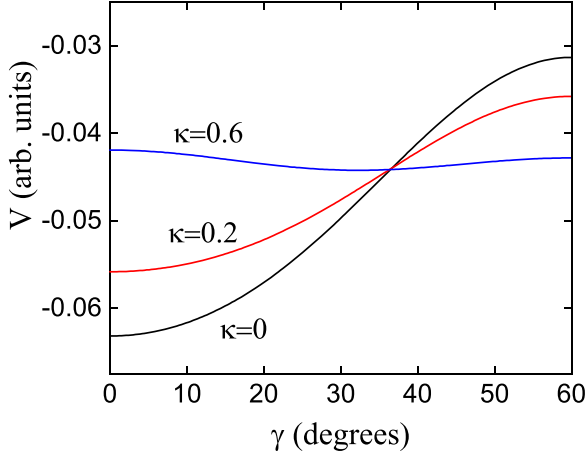


FIG. 3. Potential energy plotted as a function of γ via the minimum points marked in Fig. 2

point is around 32° , which corresponds to a typical triaxial shape. The potential curves along the γ degree of freedom via the minimum point for the three cases are shown in Fig. 3. The potential depths are 0.032, 0.020, and 0.001 for $\kappa = 0, 0.2$, and 0.6 , respectively. Although these situations do not strictly correspond to the γ -unstable mode, the potential energy surfaces exhibit very shallow minimum regions in the γ direction. This κ related shape transformation is consistent with the evolution of the quadrupole moment of the 2_1^+ state shown in Fig. 6. In the following sections, we will show that Hamiltonian (1) can provide an accurate description for the properties of the realistic γ -soft nuclei. To avoid confusion, distinguishing between the large- N limit and finite N case ($N = 6$ in this paper) is necessary, for the parameters ξ and κ under those two conditions are not the same (see Appendix). The parameter η is less sensitive to the variation of the boson number N , so it is chosen as 0.41 for consistency with that used in Sec. V.

IV. ANALYSIS OF TRANSITIONAL BEHAVIORS

The evolution behaviors of partial low-lying levels from the U(5) limit to the SU(3) limit are demonstrated in Fig. 4. In Fig. 4(a) only the second-order and fourth-order interactions of the SU(3) limit are considered. The key finding is that the quasidegeneracy can be observed in the $4_1^+, 2_2^+$ states as well as the $6_1^+, 4_2^+, 3_1^+$ states, which implies the γ softness of the spectra. In addition, it can be noticed that the 0_2^+ state is higher than the quasidegenerate doublet states $4_1^+, 2_2^+$ and intersects with the 0_3^+ state at $\eta = 0.53$ (anticrossing). The 0_3^+ state is degenerate with the $6_1^+, 4_2^+, 3_1^+$ triple states when $\eta < 0.53$ and then begins to deviate from the triple states when $\eta > 0.53$. As a comparison, the evolution behaviors of low-lying states with $\kappa = 0.2$ are given in Fig. 4(b), where we can see that the 0_2^+ and 0_3^+ states do not have intersection-like behavior any more. However, the γ softness is still maintained in the spectra, because the quasidegeneracy holds in both the double states $4_1^+, 2_2^+$ and the triple states $6_1^+, 4_2^+, 3_1^+$.

The reduced transitional rate $B(E2)$ value is an important observable for the investigation of collective behaviors.

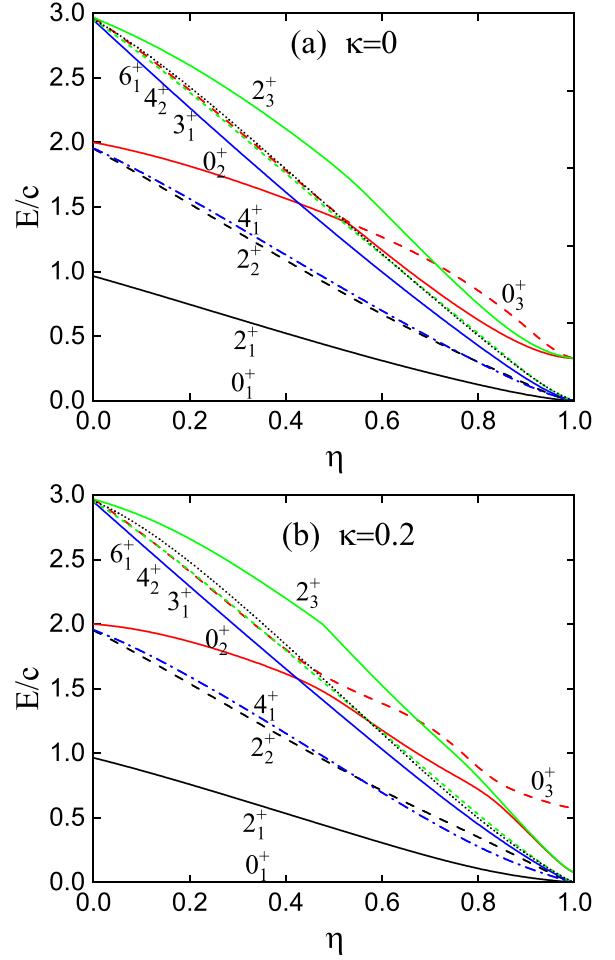


FIG. 4. Transitional behaviors of partial low-lying states as a function of η with $\xi = 0.2232$ and $N = 6$. (a) $\kappa = 0$, (b) $\kappa = 0.2$.

Usually, definite relationships between the energy spectra and the corresponding $B(E2)$ values are expected for specific nucleus. However, such relationships cannot always be maintained. For example, in Cd isotopes the energy spectra of the normal states are similar to those of the rigid spherical vibrations, but the $B(E2)$ values do not match the experimental data at all [45–49]. This demonstrates that collective behaviors cannot be solely determined by the energy spectra; the corresponding $B(E2)$ values must be considered. The $E2$ operator is defined as

$$\hat{T}(E2) = e\hat{Q}, \quad (8)$$

where e is the boson effective charge.

The transitional behaviors of the $B(E2; 2_1^+ \rightarrow 0_1^+)$, $B(E2; 0_2^+ \rightarrow 2_1^+)$, $B(E2; 0_2^+ \rightarrow 2_2^+)$, $B(E2; 0_3^+ \rightarrow 2_1^+)$, and $B(E2; 0_3^+ \rightarrow 2_2^+)$ values are plotted in Fig. 5. In Fig. 5(a), when $\kappa = 0$, slight variation is displayed on the $B(E2; 2_1^+ \rightarrow 0_1^+)$ value. However, steep changes are demonstrated on $B(E2; 0_2^+ \rightarrow 2_1^+)$, $B(E2; 0_2^+ \rightarrow 2_2^+)$, $B(E2; 0_3^+ \rightarrow 2_1^+)$, and $B(E2; 0_3^+ \rightarrow 2_2^+)$ values just at the small level anticrossing interval of the 0_2^+ and 0_3^+ states, which is similar to that from the U(5) limit to the O(6) limit [11] shown in Fig. 5(c). In Fig. 5(b), when $\kappa = 0.2$ the curve of $B(E2; 2_1^+ \rightarrow 0_1^+)$

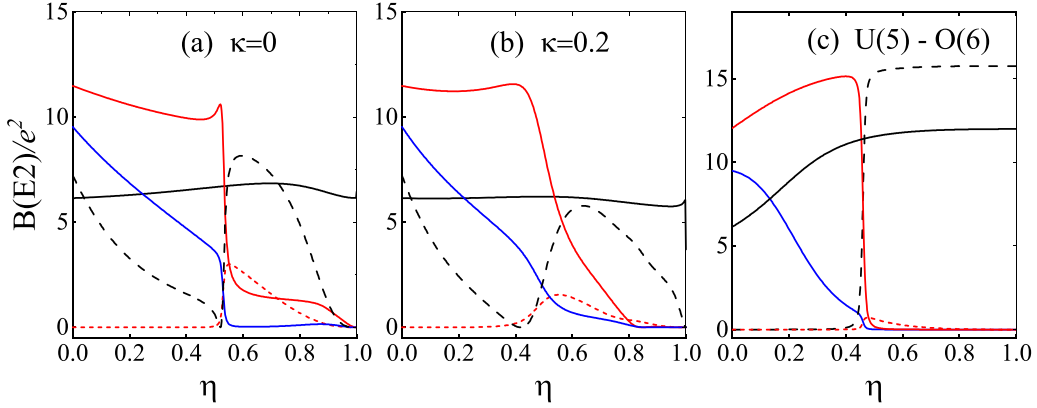


FIG. 5. Transitional behaviors of $B(E2; 2_1^+ \rightarrow 0_1^+)$ (solid black line), $B(E2; 0_2^+ \rightarrow 2_1^+)$ (solid blue line), $B(E2; 0_2^+ \rightarrow 2_2^+)$ (dashed black line), $B(E2; 0_3^+ \rightarrow 2_1^+)$ (dashed red line), and $B(E2; 0_3^+ \rightarrow 2_2^+)$ (solid red line) as a function of η for $N = 6$, (a) from the U(5) limit to the SU(3) limit with $\xi = 0.2232$ and $\kappa = 0$, (b) from the U(5) limit to the SU(3) limit with $\xi = 0.2232$ and $\kappa = 0.2$, and (c) from the U(5) limit to the O(6) limit.

value becomes flatter than the case of $\kappa = 0$. In addition, the $B(E2; 0_2^+ \rightarrow 2_1^+)$, $B(E2; 0_2^+ \rightarrow 2_2^+)$, $B(E2; 0_3^+ \rightarrow 2_1^+)$, and $B(E2; 0_3^+ \rightarrow 2_2^+)$ values no longer exhibit steep changes as those in Fig. 5(a).

TABLE I. Absolute $B(E2)$ values in W.u. for E2 transitions between the low-lying normal states in ^{82}Kr . The data of experiments, E(5), and IBM are taken from Ref. [57]. The data of DD-ME2 are taken from Ref. [61]. The Result^a and Result^b are calculated with $\kappa = 0$ and $\kappa = 0.2$, respectively. The corresponding effective charges of Result^a and Result^b are $e = 1.8037$ (W.u)^{1/2} and $e = 1.8525$ (W.u)^{1/2}, respectively. Other parameters: $\xi = 0.2232$, $\eta = 0.41$, $N = 6$.

L_i	L_f	Expt.	E(5)	IBM	DD-ME2	Result ^a	Result ^b
2_1^+	0_1^+	21.3(10)	21	21	23	21.3	21.3
4_1^+	2_1^+	31.1(31)	36	31	42	29.8	29.2
2_2^+	2_1^+	34.6(63)	36	31	24	34.6	35.8
	0_1^+	1.9(2)	0	0	0	0.14	0.45
6_1^+	4_1^+	34.3(49)	46	33	60	30.5	28.9
4_2^+	2_2^+	16.8(17)	24	17	42	16.8	17.0
	2_1^+	0.5(1)	0	0		0.26	0.44
	4_1^+	15.8(45)	22	16		17.6	18.5
3_1^+	2_1^+	1.0(2)	0	0	1	0.18	0.64
	2_2^+	27.8(72)	34	24	41	32.8	32.7
	4_1^+	9.7(75)				15.4	16.1
8_1^+	6_1^+	>23.9	54	31	85	24.8	22.1
6_2^+	4_2^+	>21.9	37	21	64	18.5	17.8
	6_1^+	>7.6	17	10		10.1	10.5
5_1^+	3_1^+	17.3(15)	28	16	54	19.5	18.9
	4_2^+	7.3(18)	13	7		12.4	11.7
0_3^+	2_1^+		0	0	10	0.02	0.84
	2_2^+		46	33	44	32.3	39.6
0_2^+	2_1^+	12.1(20)	18	12	18	15.0	13.0
	2_2^+	2.0(40)	0	0		5.0	0.05
2_3^+	0_2^+	12.7(27)	16	13	35	16.7	13.2
	2_2^+	$2.5^{+0.8}_{-1.1}$	4	2		3.2	3.1
4_3^+	2_3^+	>18.5	26	21		21.5	18.0
2_4^+	2_3^+	>20.5	26	21		21.5	19.2

If deformation is the main paradigm in nuclear structure [50], the spectroscopic quadrupole moment will be one of the most relevant quantities, especially for the prolate-oblate shape phase transition. The quadrupole moment of the 2_1^+ state is given in Fig. 6(a). It can be seen that with increasing η the values of quadrupole moment vary from negative to positive. This means that the shapes change from prolate to oblate, although they are all accompanied by a little bit deformation. In the SU(3) limit, it exhibits an oblate shape, which is induced by the fourth-order interaction $\hat{C}_2^2[\text{SU}(3)]$. It can be seen that the value of quadrupole moment with $\kappa = 0.2$ is larger than the case of $\kappa = 0$, which indicates that $\hat{C}_3[\text{SU}(3)]$ can make the nucleus more oblate. In the O(6) limit the quadrupole moment of each state is 0. Thus quadrupole moment can serve as an indicator of γ softness. As depicted in Fig. 6(b) when $\kappa = 0$ the values of $Q_{2_1^+}$, $Q_{2_2^+}$, and $Q_{4_1^+}$ are approximately 0 around $\eta = 0.6$, except for a slight deviation in $Q_{6_1^+}$. This phenomenon also indicates the O(6)-like γ softness existing in our model, which will be discussed for the nucleus of ^{196}Pt in future.

V. THEORETICAL FITTING OF ^{82}Kr

^{82}Kr has been identified experimentally as an empirical realization of E(5) features [57,65]. The partial low-lying levels of ^{82}Kr are demonstrated in Fig. 7, where (a), (b), and (c) are the energy spectra of E(5) symmetry [57], IBM calculations [57], and DD-ME2 calculations [61], respectively. The experimental results are displayed in Fig. 7(d), and our calculation results are given in Figs. 7(e) and 7(f) with the fitting point $\eta = 0.41$. It should be noticed that the parameter η used here does not corresponding to the crossing point of 0_2^+ and 0_3^+ states shown in Fig. 1(a). Because the experimental result shown in Fig. 7(d) do not exhibit the generation of 0_2^+ and 0_3^+ states, in order to be consistent with the experiment η is chosen as 0.41. The total fitting parameter c used in Figs. 7(e) and 7(f) is determined by normalizing the calculated 2_1^+ state to the experimental value. It can be seen that our calculated results reproduce the overall features of the experimental energy spectra; especially the energy levels of the 0_2^+ and 0_3^+

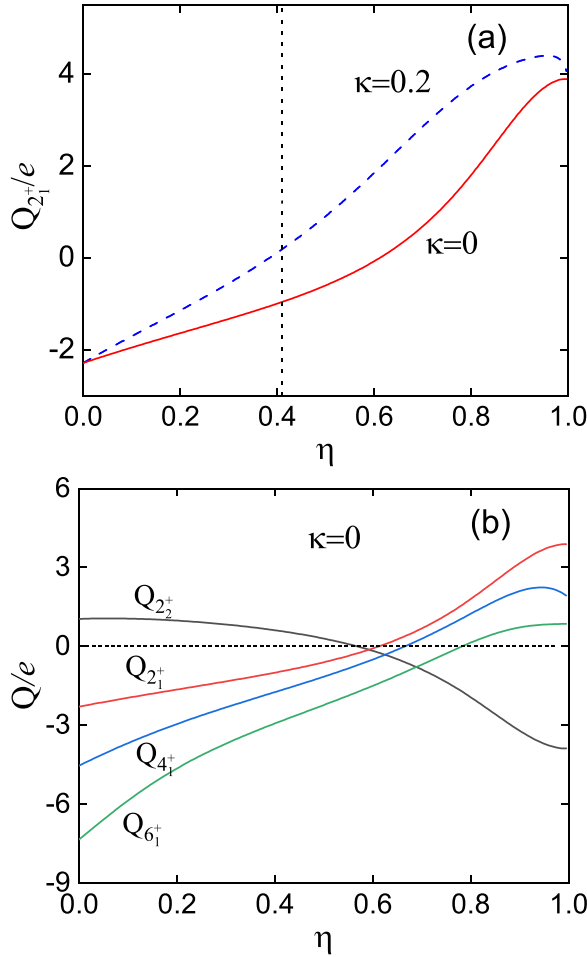


FIG. 6. (a) Transitional behaviors of the quadrupole moment of the 2_1^+ state as a function of η with $\kappa = 0$ and $\kappa = 0.2$. (b) Transitional behaviors of the quadrupole moments of 2_1^+ , 2_2^+ , 4_1^+ , and 6_1^+ states as a function of η with $\kappa = 0$. Other parameters are $N = 6$ and $\xi = 0.2232$.

fit well with the experiment data. The main drawback of our theoretical calculation is that the higher levels of 8_1^+ , 4_4^+ , and 2_4^+ are somewhat lower than the experimental results. When $\kappa = 0.2$ the energy levels of ^{82}Kr are slightly higher than the case of $\kappa = 0$. The theoretical results are expected to be better in line with the experimental results when more SU(3) higher-order interactions are considered in the Hamiltonian, and this will be investigated in future. Reference [57] shows that ^{82}Kr can be well described by E(5) symmetry. In this paper, it is shown that the E(5)-like γ softness of ^{82}Kr can be also well described by the SU3-IBM, which is the main conclusion of this paper.

The experimental and theoretical $B(E2)$ values are shown in Table I. The $B(E2)$ values between some low-lying levels of ^{82}Kr in the last two columns are calculated with $\kappa = 0$ and $\kappa = 0.2$, respectively. It can be seen that the values of the last two columns are basically identical except for those of $B(E2; 0_3^+ \rightarrow 2_1^+)$ and $B(E2; 0_2^+ \rightarrow 2_2^+)$. Compared to the experimental results in the third column [57], the calculated $B(E2; 2_2^+ \rightarrow 0_1^+)$ values for $\kappa = 0$ and $\kappa = 0.2$ are 0.14 and

0.45 W.u., respectively, which are smaller than the experimental result of 1.9 W.u., but consistent with the results of E(5) symmetry. Similar situation also occurs for the $B(E2; 3_1^+ \rightarrow 2_1^+)$ values. Besides, significant differences are displayed in the calculated $B(E2; 0_2^+ \rightarrow 2_2^+)$ values for different κ , where the calculated results are larger and smaller than the experimental results for $\kappa = 0$ and $\kappa = 0.2$, respectively. Other calculated results fit well with the experimental results, which implies that the new theory exhibits close relationships with the actual properties of ^{82}Kr and E(5) symmetry.

The predicted values of the quadrupole moment of the 2_1^+ state are -0.388 eb and 0.071 eb for $\kappa = 0$ and $\kappa = 0.2$, respectively (see Fig. 6). The former value indicates a prolate shape of the nucleus, while the latter suggests a γ -soft one with a slightly oblate shape. Although the energies of the low-lying levels and $B(E2)$ values are similar for $\kappa = 0$ and $\kappa = 0.2$, their quadrupole moments are very different due to the sensitivity of quadrupole moment to nuclear shape. Therefore, experimental measurements are awaited.

VI. CONCLUSIONS

The interacting boson model with SU(3) higher-order interactions (SU3-IBM) is used to investigate the spectroscopic properties of ^{82}Kr , which were recently identified as empirical evidence for the E(5) CPS. In previous studies [44], the Hamiltonian of the SU(3) limit only consists of the second-order Casimir operator $\hat{C}_2[\text{SU}(3)]$ and the third-order Casimir operator $\hat{C}_3[\text{SU}(3)]$. If this Hamiltonian is used to describe the properties of the typical γ -soft nucleus ^{196}Pt , large energy difference will exist between the 0_2^+ and 0_3^+ states. To overcome this difficulty, SU(3) fourth-order interaction $\hat{C}_2^2[\text{SU}(3)]$ is considered. The calculated results reveal that the energy difference of 0_2^+ and 0_3^+ states can be reduced in this new model. More importantly, the resulting transitional behaviors are similar to those from the U(5) limit to the O(6) limit. Therefore, it is expected that E(5)-like new γ softness can exist in the new model. The theoretical calculated energies and the $B(E2)$ values between the relevant states in ^{82}Kr exhibit striking agreement with the experimental results and the E(5) symmetry.

Based on these important findings, realistic γ -soft nuclei need to be further investigated in this new SU3-IBM, especially the traditional O(6)-like γ -soft nuclei, such as ^{196}Pt . Experimental investigations have revealed that the γ -soft behaviors in $^{124-132}\text{Xe}$ [66–73] and $^{98-102}\text{Zr}$ [74,75] cannot be explained using the traditional γ -soft descriptions, but can be further studied in the new model. On the other hand, it is worth noting that in the SU3-IBM there exists anticrossing between the 0_2^+ and 0_3^+ states, which is very similar to the level crossing observed in the original IBM-1 model. This implies that a systematic investigation of this structure characteristic is necessary. Besides, our results also contribute to the understanding of the prolate-oblate shape phase transition.

ACKNOWLEDGMENTS

The authors are grateful to K. Nomura for providing the data of DD-ME2 in Fig. 7(c). C.Z. gratefully acknowledges

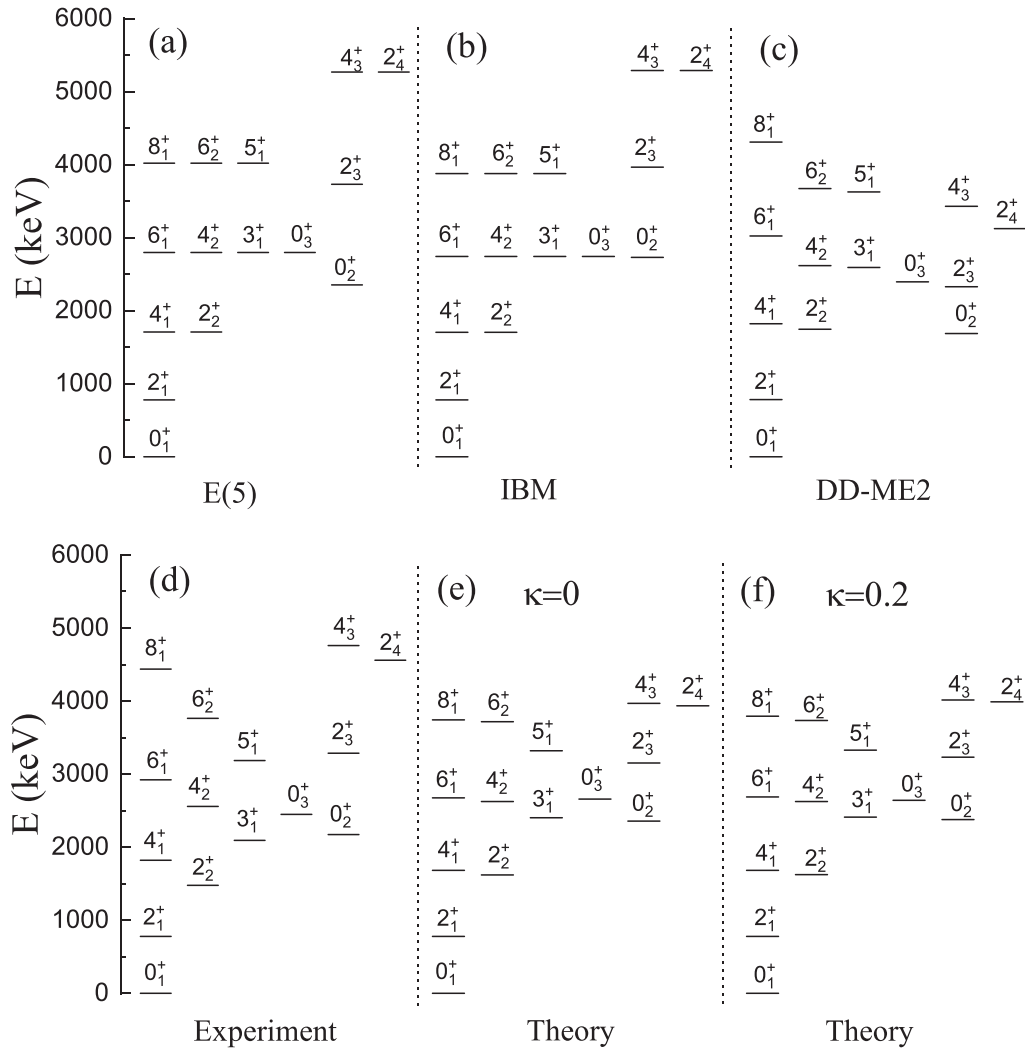


FIG. 7. The comparison of experimental and calculated partial low-lying level spectra for the ^{82}Kr nucleus. (a), (b), and (c) are the energy spectra of E(5) symmetry, IBM calculations, and DD-ME2 calculations, respectively. (d) is the experimental results. (e) and (f) are the calculation results with $\kappa = 0$, $c = 1517.4$ KeV and $\kappa = 0.2$, $c = 1486.6$ KeV, respectively. Other parameters used in (e) and (f) are $\eta = 0.41$, $\xi = 0.2232$, and $N = 6$. The data of E(5), IBM, and experiment are taken from Ref. [57]. The data of DD-ME2 are taken from Ref. [61]

support from the Scientific Research Fund of Hunan Provincial Education Department (No. 21A0427).

APPENDIX: PARAMETERS ξ AND κ

In the SU3-IBM, the SU(3) symmetry dominates the deformation of the nucleus. This possibility was first pointed out in Ref. [25], but was not taken seriously. In Ref. [44], the SU(3) second-order Casimir operator $-\hat{C}_2[\text{SU}(3)]$ and third-order Casimir operator $\hat{C}_3[\text{SU}(3)]$ are used to describe the shape phase transition from the prolate shape to the oblate shape [36]. However, in the deformation regime of the SU(3) limit, the rigid triaxial shape cannot be realized. When the U(5) limit is added, new γ -softness can emerge, but the energy of the 0_3^+ state is almost twice the one of the 0_2^+ state. Although this new mode can successfully describe the normal states of ^{110}Cd , it does not conform to the actual situation of many γ -soft nuclei.

For example, in the E(5) nuclei, the 0_2^+ and 0_3^+ states are very close.

Reference [25] pointed out that each irrep of the SU(3) symmetry corresponds to a specific deformation, such as $(2N, 0)$ for the prolate shape and $(0, N)$ for the oblate shape. If other representations can be reduced to the ground state, it is possible to achieve the rigid triaxiality. They proposed a very efficient mechanism by introducing SU(3) fourth-order interaction $\hat{C}_2^2[\text{SU}(3)]$, which corresponds to the formalism

$$\hat{H}_1 = c \left[-\frac{\hat{C}_2[\text{SU}(3)]}{2N} + \kappa \frac{\hat{C}_3[\text{SU}(3)]}{2N^2} + \xi \frac{\hat{C}_2^2[\text{SU}(3)]}{2N^3} \right]. \quad (\text{A1})$$

Then the energy of Eq. (A1) for the irrep (λ, μ) is

$$E_1(\lambda, \mu) = c \left[-\frac{g(\lambda, \mu)}{2N} + \kappa \frac{h(\lambda, \mu)}{2N^2} + \xi \frac{g(\lambda, \mu)^2}{2N^3} \right], \quad (\text{A2})$$

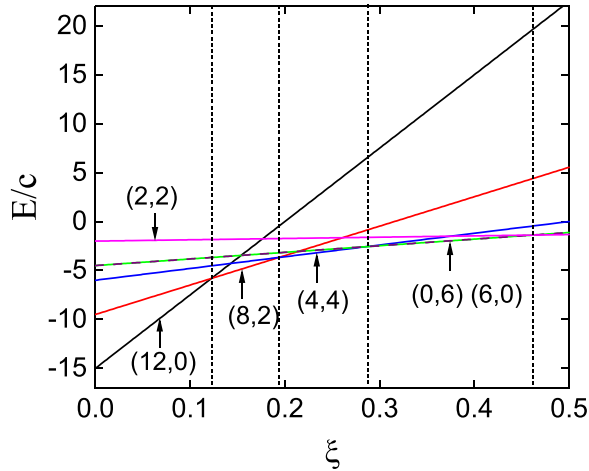


FIG. 8. The six lowest 0^+ levels with specific (λ, μ) as a function of ξ with $\kappa = 0$ in the SU(3) limit.

where $g(\lambda, \mu) = \langle \hat{C}_2[\text{SU}(3)] \rangle = \lambda^2 + \mu^2 + \lambda\mu + 3\lambda + 3\mu$ and $h(\lambda, \mu) = \langle \hat{C}_3[\text{SU}(3)] \rangle = \frac{1}{9}(\lambda - \mu)(2\lambda + \mu + 3)(\lambda + 2\mu + 3)$. Thus, if the irrep (λ_0, μ_0) is the ground state, it satisfies the condition

$$\xi = \frac{N^2}{2g(\lambda_0, \mu_0)} - \frac{\kappa N}{6g(\lambda_0, \mu_0)}(3 + \lambda_0 + 2\mu_0), \quad (\text{A3})$$

which is obtained by calculating the derivatives of formula (A2) and can be used to choose the value of ξ .

To reduce the energy difference between the 0_2^+ and 0_3^+ states, the previous IBM-1 can give us some inspiration. In the transitional behaviors from the U(5) limit to the O(6) limit, there exists a crossover phenomenon between the 0_2^+ and 0_3^+ states [11]. The O(6) limit corresponds to the γ -unrelated case, where the average value of the γ degree of freedom is $\gamma_{\text{eff}} = 30^\circ$. In the SU3-IBM, this implies that the shape in the SU(3) limit is a rigid triaxial deformation with $\gamma = 30^\circ$. The value of the quadrupole shape variable γ for the SU(3) irrep (λ_0, μ_0) in the finite- N case can be expressed as [36]

$$\gamma = \tan^{-1} \left(\frac{\sqrt{3}(\mu_0 + 1)}{2\lambda_0 + \mu_0 + 3} \right). \quad (\text{A4})$$

Obviously, $\gamma = 30^\circ$ if $\lambda_0 = \mu_0$, which is valid in the large- N limit [26,36]. This means that the irrep of the ground state should be (λ_0, λ_0) , which can be realized by introducing the fourth-order interaction $\hat{C}_2^2[\text{SU}(3)]$. If the irrep (λ_0, λ_0) does not exist, then ξ that can result in $\gamma_{\text{eff}} = 30^\circ$ will be chosen. For example, if $N = 7$, ξ is located between the irreps (6,4) and (2,6).

To further elucidate the relationship between the SU(3) irreps of the ground state and the parameter ξ , Fig. 8 presents evolutionary behaviors of the six lowest 0^+ levels with specific irreps (λ, μ) as a function of ξ in the SU(3) limit with $\kappa = 0$. By setting the energy of the ground states to 0, Fig. 8 can

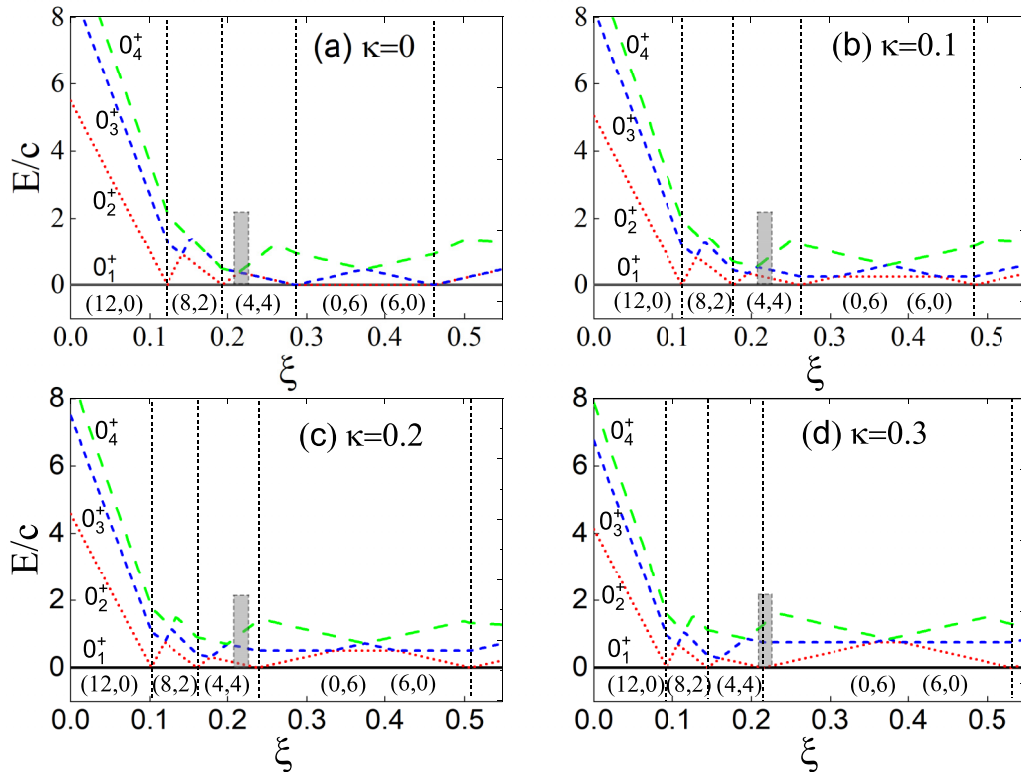


FIG. 9. Transitional behaviors of the four lowest 0^+ states are plotted as a function of ξ in the SU(3) limit, with (a) $\kappa = 0$, (b) $\kappa = 0.1$, (c) $\kappa = 0.2$, and (d) $\kappa = 0.3$. The ground states corresponding to SU(3) irreps (12,0), (8,2), (4,4) and (0,6) (6,0) for $N = 6$ are separated by dashed lines.

be represented by Fig. 9(a), which offers a more effective illustration of changes in the SU(3) irreps of the ground state. The same procedure is also employed for the cases of $\kappa = 0.1, 0.2,$ and $0.3,$ yielding Figs. 9(b), 9(c), and 9(d), respectively.

For simplicity, only the four lowest 0^+ states are plotted in Fig. 9. It can be seen that the irreps of the ground state gradually appear, with the first four labeled as (12,0), (8,2), (4,4) and (0,6) (6,0), respectively, which are separated by the dashed lines. For (12,0) and (0,6), $\gamma = 3.67^\circ$ and $\gamma = 53.41^\circ$, which correspond to the prolate and oblate deformation, respectively. For (8,2) and (4,4), $\gamma = 18.90^\circ$ and $\gamma = 30^\circ$ respectively, which represent the triaxial rotation. According to Eq. (A3), the values of ξ for the first four irreps are located at 0.1, 0.16, 0.25, and 0.33, which fall within the regions (0, 0.1225), (0.1225, 0.1925), (0.1925, 0.285), and (0.285, 0.4625) respectively in Fig. 9(a). The transitional behaviors from the U(5) limit to the SU(3) limit for Hamiltonian (1) are discussed in the vicinity of $\xi = 0.25,$ and the crossover phenomenon between the 0_2^+ and 0_3^+ state can be found for $\xi = 0.2232$ in Fig. 1.

According to Eq. (A3), for a specific irrep (λ_0, μ_0) the value of ξ decreases as κ increases. For example, when considering irrep (4,4), the values of ξ are 0.250, 0.229, 0.208, and 0.188 for $\kappa = 0, 0.1, 0.2,$ and $0.3,$ respectively. To demonstrate the effect of $\kappa,$ a gray area around 0.2232 is labeled in Fig. 9. As κ increases from 0 to 0.3, the irrep (4,4) shifts out of the gray area and the oblate deformation (0,6) moves into this region, indicating that the shape evolves from the rigid triaxial rotor to the oblate rotation. This may be affected by the (6,0) irrep, which is degenerate with (0,6). This phenomenon is consistent with the conclusion given in Ref. [36] that the SU(3) third-order interaction can induce the oblate deformation. Besides, it can be also noticed that the level interval between 0_2^+ and 0_3^+ states in the gray area becomes larger as κ increases. When choosing the value of $\kappa,$ we expect the gray area investigated in this paper to fall within the rigid triaxial deformation region of irrep (4,4), and the energy interval of 0_2^+ and 0_3^+ states in the gray area is not too large. Thus in this paper we choose $\kappa = 0$ and 0.2 for comparison.

-
- [1] A. Bohr and B. Mottelson, *Nuclear Structure, Volume II: Nuclear Deformations* (W. A. Benjamin, New York, 1975).
- [2] G. Scharff-Goldhaber and J. Weneser, System of even-even nuclei, *Phys. Rev.* **98**, 212 (1955).
- [3] A. Bohr and B. R. Mottelson, Rotational states in even-even nuclei, *Phys. Rev.* **90**, 717 (1953).
- [4] L. Willets and M. Jean, Surface oscillations in even-even nuclei, *Phys. Rev.* **102**, 788 (1956).
- [5] A. Davydov and G. Filippov, Rotational states in even atomic nuclei, *Nucl. Phys.* **8**, 237 (1958).
- [6] F. Iachello and A. Arima, *The Interacting Boson Model* (Cambridge University Press, Cambridge, 1987).
- [7] P. Cejnar, S. Heinze, and J. Jolie, Ground-state shape phase transitions in nuclei: Thermodynamic analogy and finite- N effects, *Phys. Rev. C* **68**, 034326 (2003).
- [8] R. Casten, Shape phase transitions and critical-point phenomena in atomic nuclei, *Nat. Phys.* **2**, 811 (2006).
- [9] Y. A. Luo, F. Pan, T. Wang, P. Z. Ning, and J. P. Draayer, Vibration-rotation transitional patterns in the SD -pair shell model, *Phys. Rev. C* **73**, 044323 (2006).
- [10] R. F. Casten and E. A. McCutchan, Quantum phase transitions and structural evolution in nuclei, *J. Phys. G: Nucl. Part. Phys.* **34**, R285 (2007).
- [11] F. Pan, T. Wang, Y. Huo, and J. Draayer, Quantum phase transitions in the consistent-Q Hamiltonian of the interacting boson model, *J. Phys. G: Nucl. Part. Phys.* **35**, 125105 (2008).
- [12] Y. Luo, Y. Zhang, X. Meng, F. Pan, and J. P. Draayer, Quantum phase transitional patterns in the SD -pair shell model, *Phys. Rev. C* **80**, 014311 (2009).
- [13] R. Casten, Quantum phase transitions and structural evolution in nuclei, *Prog. Part. Nucl. Phys.* **62**, 183 (2009).
- [14] P. Cejnar, J. Jolie, and R. F. Casten, Quantum phase transitions in the shapes of atomic nuclei, *Rev. Mod. Phys.* **82**, 2155 (2010).
- [15] J. Kotila, K. Nomura, L. Guo, N. Shimizu, and T. Otsuka, Shape phase transitions in the interacting boson model: Phenomenological versus microscopic descriptions, *Phys. Rev. C* **85**, 054309 (2012).
- [16] R. V. Jolos and E. A. Kolganova, Phase transitions in atomic nuclei, *Phys. Usp.* **64**, 325 (2021).
- [17] L. Fortunato, Quantum phase transitions in algebraic and collective models of nuclear structure, *Prog. Part. Nucl. Phys.* **121**, 103891 (2021).
- [18] F. Iachello, Dynamic Symmetries at the Critical Point, *Phys. Rev. Lett.* **85**, 3580 (2000).
- [19] F. Iachello, Analytic Description of Critical Point Nuclei in a Spherical-Axially Deformed Shape Phase Transition, *Phys. Rev. Lett.* **87**, 052502 (2001).
- [20] J. E. García-Ramos and J. M. Arias, Relation between E(5) models and the interacting boson model, *Phys. Rev. C* **77**, 054307 (2008).
- [21] F. Pan, Y. Zhang, H.-C. Xu, L.-R. Dai, and J. P. Draayer, Alternative solvable description of the E(5) critical point symmetry in the interacting boson model, *Phys. Rev. C* **91**, 034305 (2015).
- [22] P. Van Isacker and J.-Q. Chen, Classical limit of the interacting boson Hamiltonian, *Phys. Rev. C* **24**, 684 (1981).
- [23] K. Heyde, P. Van Isacker, M. Waroquier, and J. Moreau, Triaxial shapes in the interacting boson model, *Phys. Rev. C* **29**, 1420 (1984).
- [24] G. Vanden Berghe, H. E. De Meyer, and P. Van Isacker, Symmetry-conserving higher-order interaction terms in the interacting boson model, *Phys. Rev. C* **32**, 1049 (1985).
- [25] Y. F. Smirnov, N. A. Smirnova, and P. Van Isacker, SU(3) realization of the rigid asymmetric rotor within the interacting boson model, *Phys. Rev. C* **61**, 041302(R) (2000).
- [26] Y. Zhang, F. Pan, L.-R. Dai, and J. P. Draayer, Triaxial rotor in the SU(3) limit of the interacting boson model, *Phys. Rev. C* **90**, 044310 (2014).
- [27] G. Rosensteel and D. Rowe, On the shape of deformed nuclei, *Ann. Phys. (NY)* **104**, 134 (1977).

- [28] J. P. Draayer and G. Rosensteel, U(3) \rightarrow R(3) integrity-basis spectroscopy, *Nucl. Phys. A* **439**, 61 (1985).
- [29] O. Castaños, J. P. Draayer, and Y. Leschber, Shape variables and the shell model, *Z. Phys. A* **329**, 33 (1988).
- [30] J. P. Elliott, J. A. Evans, and P. Van Isacker, Definition of the Shape Parameter γ in the Interacting-Boson Model, *Phys. Rev. Lett.* **57**, 1124 (1986).
- [31] V. Kota, *SU(3) Symmetry in Atomic Nuclei* (Springer, Berlin, 2020).
- [32] J. E. García-Ramos, A. Leviatan, and P. Van Isacker, Partial Dynamical Symmetry in Quantum Hamiltonians with Higher-Order Terms, *Phys. Rev. Lett.* **102**, 112502 (2009).
- [33] A. Leviatan, Partial dynamical symmetries, *Prog. Part. Nucl. Phys.* **66**, 93 (2011).
- [34] A. Leviatan, J. E. García-Ramos, and P. Van Isacker, Partial dynamical symmetry as a selection criterion for many-body interactions, *Phys. Rev. C* **87**, 021302(R) (2013).
- [35] L. Fortunato, C. E. Alonso, J. M. Arias, J. E. García-Ramos, and A. Vitturi, Phase diagram for a cubic- Q interacting boson model hamiltonian: Signs of triaxiality, *Phys. Rev. C* **84**, 014326 (2011).
- [36] Y. Zhang, F. Pan, Y.-X. Liu, Y.-A. Luo, and J. P. Draayer, Analytically solvable prolate-oblate shape phase transitional description within the SU(3) limit of the interacting boson model, *Phys. Rev. C* **85**, 064312 (2012).
- [37] T. Grahn, S. Stolze, D. T. Joss, R. D. Page, B. Saygı, D. O'Donnell, M. Akmali, K. Andgren, L. Bianco, D. M. Cullen, A. Dewald, P. T. Greenlees, K. Heyde, H. Iwasaki, U. Jakobsson, P. Jones, D. S. Judson, R. Julin, S. Juutinen, S. Ketelhut *et al.*, Excited states and reduced transition probabilities in ^{168}Os , *Phys. Rev. C* **94**, 044327 (2016).
- [38] B. Saygı, D. T. Joss, R. D. Page, T. Grahn, J. Simpson, D. O'Donnell, G. Alharshan, K. Auranen, T. Bäck, S. Boening, T. Braunroth, R. J. Carroll, B. Cederwall, D. M. Cullen, A. Dewald, M. Doncel, L. Donosa, M. C. Drummond, F. Ertuğral, S. Ertürk *et al.*, Reduced transition probabilities along the yrast line in ^{166}W , *Phys. Rev. C* **96**, 021301 (2017).
- [39] B. Cederwall, M. Doncel, O. Aktas, A. Ertoprak, R. Liotta, C. Qi, T. Grahn, D. M. Cullen, B. S. Nara Singh, D. Hodge, M. Giles, S. Stolze, H. Badran, T. Braunroth, T. Calverley, D. M. Cox, Y. D. Fang, P. T. Greenlees, J. Hilton, E. Ideguchi *et al.*, Lifetime Measurements of Excited States in ^{172}Pt and the Variation of Quadrupole Transition Strength with Angular Momentum, *Phys. Rev. Lett.* **121**, 022502 (2018).
- [40] A. Goasduff, J. Ljungvall, T. R. Rodríguez, F. L. Bello Garrote, A. Etile, G. Georgiev, F. Giacoppo, L. Grente, M. Klintefjord, A. Kuşoğlu, I. Matea, S. Rocca, M.-D. Salsac, and C. Sotty, $B(E2)$ anomalies in the yrast band of ^{170}Os , *Phys. Rev. C* **100**, 034302 (2019).
- [41] T. Wang, $B(E2)$ anomaly cannot be explained with O(6) higher-order interactions, *Phys. Rev. C* **107**, 064303 (2023).
- [42] T. Wang, A collective description of the unusually low ratio $B_{4/2} = B(E2; 4_1^+ \rightarrow 2_1^+)/B(E2; 2_1^+ \rightarrow 0_1^+)$, *Europhys. Lett.* **129**, 52001 (2020).
- [43] Y. Zhang, Y.-W. He, D. Karlsson, C. Qi, F. Pan, and J. Draayer, A theoretical interpretation of the anomalous reduced E2 transition probabilities along the yrast line of neutron-deficient nuclei, *Phys. Lett. B* **834**, 137443 (2022).
- [44] T. Wang, New γ -soft rotation in the interacting boson model with SU(3) higher-order interactions, *Chin. Phys. C* **46**, 074101 (2022).
- [45] P. E. Garrett, K. L. Green, and J. L. Wood, Breakdown of vibrational motion in the isotopes $^{110-116}\text{Cd}$, *Phys. Rev. C* **78**, 044307 (2008).
- [46] P. Garrett and J. Wood, On the robustness of surface vibrational modes: case studies in the Cd region, *J. Phys. G: Nucl. Part. Phys.* **37**, 064028 (2010).
- [47] K. Heyde and J. L. Wood, Shape coexistence in atomic nuclei, *Rev. Mod. Phys.* **83**, 1467 (2011).
- [48] P. E. Garrett, J. Bangay, A. Diaz Varela, G. C. Ball, D. S. Cross, G. A. Demand, P. Finlay, A. B. Garnsworthy, K. L. Green, G. Hackman, C. D. Hannant, B. Jigmeddorj, J. Jolie, W. D. Kulp, K. G. Leach, J. N. Orce, A. A. Phillips, A. J. Radich, E. T. Rand, M. A. Schumaker *et al.*, Detailed spectroscopy of ^{110}Cd : Evidence for weak mixing and the emergence of γ -soft behavior, *Phys. Rev. C* **86**, 044304 (2012).
- [49] J. C. Batchelder, N. T. Brewer, R. E. Goans, R. Grzywacz, B. O. Griffith, C. Jost, A. Korgul, S. H. Liu, S. V. Paulauskas, E. H. Spejewski, and D. W. Stracener, Low-lying collective states in ^{120}Cd populated by β decay of ^{120}Ag : Breakdown of the anharmonic vibrator model at the three-phonon level, *Phys. Rev. C* **86**, 064311 (2012).
- [50] K. Heyde and J. Wood, Nuclear shapes: from earliest ideas to multiple shape coexisting structures, *Phys. Scr.* **91**, 083008 (2016).
- [51] P. Garrett, J. Wood, and S. Yates, Critical insights into nuclear collectivity from complementary nuclear spectroscopic methods, *Phys. Scr.* **93**, 063001 (2018).
- [52] P. E. Garrett, T. R. Rodríguez, A. D. Varela, K. L. Green, J. Bangay, A. Finlay, R. A. E. Austin, G. C. Ball, D. S. Bandyopadhyay, V. Bildstein, S. Colosimo, D. S. Cross, G. A. Demand, P. Finlay, A. B. Garnsworthy, G. F. Grinyer, G. Hackman, B. Jigmeddorj, J. Jolie, W. D. Kulp *et al.*, Multiple Shape Coexistence in $^{110-112}\text{Cd}$, *Phys. Rev. Lett.* **123**, 142502 (2019).
- [53] P. E. Garrett, T. R. Rodríguez, A. Diaz Varela, K. L. Green, J. Bangay, A. Finlay, R. A. E. Austin, G. C. Ball, D. S. Bandyopadhyay, V. Bildstein, S. Colosimo, D. S. Cross, G. A. Demand, P. Finlay, A. B. Garnsworthy, G. F. Grinyer, G. Hackman, B. Jigmeddorj, J. Jolie, W. D. Kulp *et al.*, Shape coexistence and multiparticle-multihole structures in $^{110-112}\text{Cd}$, *Phys. Rev. C* **101**, 044302 (2020).
- [54] T. Wang, B. C. He, C. X. Zhou, D. K. Li, and L. Fortunato, Emerging γ -softness in ^{196}Pt in the SU3-IBM (unpublished).
- [55] T. Wang, B. C. He, D. K. Li, and C. X. Zhou, Prolate-oblate asymmetric shape phase transition in the interacting boson model with SU(3) higher-order interactions, *Phys. Rev. C* **107**, 064322 (2023).
- [56] K. Kaneko, Y. Sun, N. Shimizu, and T. Mizusaki, Quasi-SU(3) Coupling Induced Oblate-Prolate Shape Phase Transition in the Casten Triangle, *Phys. Rev. Lett.* **130**, 052501 (2023).
- [57] S. Rajbanshi, S. Bhattacharya, R. Raut, R. Palit, S. Ali, R. Santra, H. Pai, F. S. Babra, R. Banik, S. Bhattacharyya, P. Dey, G. Mukherjee, M. S. R. Laskar, S. Nandi, T. Trivedi, S. S. Ghugre, and A. Goswami, Experimental evidence of exact E(5) symmetry in ^{82}Kr , *Phys. Rev. C* **104**, L031302 (2021).
- [58] E. López-Moreno and O. Castaños, Shapes and stability within the interacting boson model: Dynamical symmetries, *Phys. Rev. C* **54**, 2374 (1996).
- [59] J. Jolie, R. F. Casten, P. von Brentano, and V. Werner, Quantum Phase Transition for γ -Soft Nuclei, *Phys. Rev. Lett.* **87**, 162501 (2001).

- [60] J. Jolie and A. Linnemann, Prolate-oblate phase transition in the Hf-Hg mass region, *Phys. Rev. C* **68**, 031301(R) (2003).
- [61] K. E. Karakatsanis and K. Nomura, Signatures of shape phase transitions in krypton isotopes based on relativistic energy density functionals, *Phys. Rev. C* **105**, 064310 (2022).
- [62] D. J. Rowe, Microscopic theory of the nuclear collective model, *Rep. Prog. Phys.* **48**, 1419 (1985).
- [63] J. M. Arias, J. Dukelsky, and J. E. García-Ramos, Quantum Phase Transitions in the Interacting Boson Model: Integrability, Level Repulsion, and Level Crossing, *Phys. Rev. Lett.* **91**, 162502 (2003).
- [64] N. V. Zamfir, P. von Brentano, R. F. Casten, and J. Jolie, Test of two-level crossing at the $N = 90$ spherical-deformed critical point, *Phys. Rev. C* **66**, 021304(R) (2002).
- [65] Y. Zhang, Z.-T. Wang, H.-D. Jiang, and X. Chen, Hidden euclidean dynamical symmetry in the $U(n+1)$ vibron model, *Symmetry* **14**, 2219 (2022).
- [66] L. Coquard, N. Pietralla, T. Ahn, G. Rainovski, L. Bettermann, M. P. Carpenter, R. V. F. Janssens, J. Leske, C. J. Lister, O. Möller, W. Rother, V. Werner, and S. Zhu, Robust test of E(5) symmetry in ^{128}Xe , *Phys. Rev. C* **80**, 061304(R) (2009).
- [67] G. Rainovski, N. Pietralla, T. Ahn, L. Coquard, C. Lister, R. Janssens, M. Carpenter, S. Zhu, L. Bettermann, J. Jolie, W. Rother, R. Jolos, and V. Werner, How close to the O(6) symmetry is the nucleus ^{124}Xe ? *Phys. Lett. B* **683**, 11 (2010).
- [68] L. Coquard, G. Rainovski, N. Pietralla, T. Ahn, L. Bettermann, M. P. Carpenter, R. V. F. Janssens, J. Leske, C. J. Lister, O. Möller, T. Möller, W. Rother, V. Werner, and S. Zhu, O(6)-symmetry breaking in the γ -soft nucleus ^{126}Xe and its evolution in the light stable xenon isotopes, *Phys. Rev. C* **83**, 044318 (2011).
- [69] E. E. Peters, T. J. Ross, S. F. Ashley, A. Chakraborty, B. P. Crider, M. D. Hennek, S. H. Liu, M. T. McEllistrem, S. Mukhopadhyay, F. M. Prados-Estévez, A. P. D. Ramirez, J. S. Thrasher, and S. W. Yates, 0^+ states in $^{130-132}\text{Xe}$: A search for E(5) behavior, *Phys. Rev. C* **94**, 024313 (2016).
- [70] E. E. Peters, A. E. Stuchbery, A. Chakraborty, B. P. Crider, S. F. Ashley, A. Kumar, M. T. McEllistrem, F. M. Prados-Estévez, and S. W. Yates, Emerging collectivity from the nuclear structure of ^{132}Xe : Inelastic neutron scattering studies and shell-model calculations, *Phys. Rev. C* **99**, 064321 (2019).
- [71] L. Morrison, K. Hadyńska-Klęk, Z. Podolyák, D. T. Doherty, L. P. Gaffney, L. Kaya, L. Próchniak, J. Samorajczyk-Pyšk, J. Srebny, T. Berry, A. Boukhari, M. Brunet, R. Canavan, R. Catherall, S. J. Colosimo, J. G. Cubiss, H. De Witte, C. Fransen, E. Giannopoulos, H. Hess *et al.*, Quadrupole deformation of ^{130}Xe measured in a Coulomb-excitation experiment, *Phys. Rev. C* **102**, 054304 (2020).
- [72] S. Kisyov, C. Y. Wu, J. Henderson, A. Gade, K. Kaneko, Y. Sun, N. Shimizu, T. Mizusaki, D. Rhodes, S. Biswas, A. Chester, M. Devlin, P. Farris, A. M. Hill, J. Li, E. Rubino, and D. Weisshaar, Structure of $^{126-128}\text{Xe}$ studied in Coulomb excitation measurements, *Phys. Rev. C* **106**, 034311 (2022).
- [73] E. Clément, A. Lemasson, M. Rejmund, B. Jacquot, D. Ralet, C. Michelagnoli, D. Barrientos, P. Bednarczyk, G. Benzoni, A. J. Boston, A. Bracco, B. Cederwall, M. Ciemala, J. Collado, F. Crespi, C. Domingo-Pardo, J. Dudouet, H. J. Eberth, G. de France, A. Gadea *et al.*, Spectroscopic quadrupole moments in ^{124}Xe , *Phys. Rev. C* **107**, 014324 (2023).
- [74] W. Urban, T. Rząca-Urban, J. Wiśniewski, A. G. Smith, G. S. Simpson, and I. Ahmad, First observation of γ -soft and triaxial bands in Zr isotopes, *Phys. Rev. C* **100**, 014319 (2019).
- [75] V. Karayonchev, J. Jolie, A. Blazhev, A. Dewald, A. Esmaylzadeh, C. Fransen, G. Häfner, L. Knafka, J. Litzinger, C. Müller-Gatermann, J.-M. Régis, K. Schomacker, A. Vogt, N. Warr, A. Leviatan, and N. Gavrielov, Tests of collectivity in ^{98}Zr by absolute transition rates, *Phys. Rev. C* **102**, 064314 (2020).